A Patch-Clamp Study on the Physiology of Aluminum Toxicity and Aluminum Tolerance in Maize. Identification and Characterization of Al^{3+}-Induced Anion Channels[1]

Miguel A. Piñeros and Leon V. Kochian*

United States Plant, Soil, and Nutrition Laboratory, United States Department of Agriculture, Agricultural Research Service, Cornell University, Ithaca, New York 14853

The presence of Al^{3+} in the rhizosphere induces citrate efflux from the root apex of the Al-tolerant maize (*Zea mays*) hybrid South American 3, consequently chelating and reducing the activity of toxic Al^{3+} at the root surface. Because citrate is released from root apical cells as the deprotonated anion, we used the patch-clamp technique in protoplasts isolated from the terminal 5 mm of the root to study the plasma membrane ion transporters that could be involved in Al-tolerance and Al-toxicity responses. Acidification of the extracellular environment stimulated inward K^+ currents while inhibiting outward K^+ currents. Addition of extracellular Al^{3+} inhibited the remaining K^+ outward currents, blocked the K^+ inward current, and caused the activation of an inward Cl^- current (anion efflux). Studies with excised membrane patches revealed the existence of Al-dependent anion channels, which were highly selective for anions over cations. Our success in activating this channel with extracellular Al^{3+} in membrane patches excised prior to any Al^{3+} exposure indicates that the machinery required for Al^{3+} activation of this channel, and consequently the whole root Al^{3+} response, is localized to the root-cell plasma membrane. This Al^{3+}-activated anion channel may also be permeable to organic acids, thus mediating the Al-tolerance response (i.e. Al-induced organic acid exudation) observed in intact maize root apices.

Al limits the agricultural productivity on approximately 30% of the world's total land area, as the rhizotoxic species Al^{3+} solubilizes into acid soil solutions, accumulating to levels that inhibit root growth and function. However, plants have evolved tolerance mechanisms enabling them to grow in soil environments where the roots are exposed to potentially high levels of Al (for review, see Kochian, 1995). Identification of Al-induced organic acid release by the root apex of Al-tolerant genotypes provided the first compelling evidence for the existence of such a tolerance mechanism, where the exuded organic acids chelate and reduce the activities of toxic Al^{3+} in the rhizosphere (Delhaize et al., 1993a, 1993b). Al-induced exudation of several different organic acids has been described from roots of a variety of Al-tolerant plant species: malate being released in wheat (*Triticum aestivum*; Ryan et al., 1995b; Pellet et al., 1996), citrate in maize (*Zea mays*) and *Cassia tora* (Pellet et al., 1995; Ma et al., 1997b), and oxalate in buckwheat and taro (Ma et al., 1997a; Ma and Miyasaka, 1998; Zheng et al., 1998). Given the neutral pH of the cytoplasm, organic acids in the cytoplasm are largely deprotonated and exist as anions. Since the equilibrium potential for organic acid anions (as well as inorganic anions) is much more positive than that of the resting membrane potential in root cells, activation (i.e. opening) of plasma membrane anion channels will result in a large anion efflux down the outward electrochemical gradient. Thus, it is likely that anion channels (permeable to organic acids) will constitute the transport mechanism via which Al-induced organic acid exudation occurs. In support of this, Ryan et al. (1997) reported an anion channel in protoplasts isolated from root tips of Al-tolerant wheat, which was specifically activated by extracellular Al^{3+}. In addition to this ligand-gated channel, several plasma membrane anion-permeable channels have also been identified in other higher plant tissues. Voltage gated anion channels have been reported in protoplasts derived from different tissues such as root cortical (Skerrett and Tyerman, 1994; Tyerman et al., 1997) and xylem parenchyma cells (Wegner and Raschke, 1994; Köhler and Raschke, 2000), hypocotyl epidermal cells (Thomine et al., 1995), guard cells (Schroeder and Hagiwara, 1989; Schroeder and Keller, 1992), and suspension cells (Zimmermann et al., 1994; Amtmann et al., 1997). Mechanically gated-anion permeable channels (e.g. stretch activated) have also been reported in the plasma membrane of guard cells (Cosgrove and Hedrich, 1991).

Anion channels are involved in a wide range of physiological responses such as regulation of stomatal conductance, stabilization of membrane potential, nutrient transport, and turgor adjustment (Tyerman,

1992; Schroeder, 1995). Although these anion channels share many similarities, there are also significant differences in their biophysical properties. For example although most anion channels catalyze anion efflux as they open upon membrane depolarization, anion channels activating at hyperpolarized membrane potentials or mediating anion influx have also been reported (Terry et al., 1991; Skerrett and Tyerman, 1994). Also, a wide range of intracellular and extracellular factors can modulate the activity of many of these channels. The ionic environment surrounding the channel (e.g. intracellular and extracellular Ca^{2+} activities, as well as the extracellular concentration of other ions) has been shown to influence the permeation of anions through some of these channels (Schroeder and Hagiwara, 1989; Hedrich et al., 1990; Skerrett and Tyerman, 1994; Schulz-Lessdorf et al., 1996; Tyerman et al., 1997; Köhler and Raschke, 2000). Endogenous signals (e.g. auxins), as well as changes in the channel's phosphorylation state may also be involved in the modulation of channel activity (Hedrich et al., 1990; Zimmermann et al., 1994; Schmidt et al., 1995; Schulz-Lessdorf et al., 1996; Thomine et al., 1997).

These biophysical and regulatory differences point to the existence of several types of anion channels with diverse physiological roles in vivo. We have made use of the patch-clamp technique (Hamill et al., 1981) to gain insight into the influence of extracellular Al^{3+} on some of the plasma membrane ion transporters of root apical cells of the Al-tolerant maize hybrid South American 3, as the root apex is considered to be critical in both Al-toxicity and Al-tolerance responses in crop plants (Ryan et al., 1993; Kochian, 1995).

RESULTS

Whole-Cell Conductances for Protoplasts from the Maize Root Apex

The protoplasts isolated from the root apex (first 5 mm of the root) of the Al-tolerant maize hybrid South American 3 were mainly a mixture of meristematic, cortical, and stelar protoplasts that were morphologically distinguishable. Visual examinations of the partially digested tissue showed that neither root cap nor epidermal cells were digested. According to the morphology described for maize root protoplasts (Roberts and Tester, 1995), most cells selected for the present study were likely to be cortex protoplasts with a diameter of 35 to 50 μm, containing large vacuoles and relatively little cytoplasm. In contrast with the success we had in obtaining high-resistance seals in protoplasts from the mature root region, protoplasts isolated from the root tip proved to be more delicate, allowing occasional (1 of every 8 attempts) formation of high resistance seals (3 GΩ in average). A total of 89 cells was examined under experimental conditions where the cell's cytoplasmic

solution (i.e. the solution inside the patch pipette) and bath solution contained physiologically relevant K$^+$ activities at different pH values. Under these conditions three main types of currents co-existed in the plasma membrane of root tip protoplasts (Fig. 1, A and B). At depolarizing potentials the whole-cell conductance of most cells (74%) was dominated by an instantaneous K$^+$ outward current. This current developed rapidly, reaching a steady magnitude within 100 ms with activation constants decreasing from 25 to 5 ms (in sealing solution) as the holding potential became more positive (from 30–100 mV). Similar instantaneous K$^+$ outward currents have been reported for mature maize root cells (Roberts and Tester, 1995), as well as for root parenchyma (Wegner and De Boer, 1997), cotyledonary tissue (Terry et al., 1992), and mesophyll (M.A. Piñeros, L.V. Kochian, unpublished data) cells from other plant species. A small fraction of the cells (23%) displayed a time-dependent K$^+$ inward rectifier at hyperpolarizing holding potentials, whereas in a smaller fraction (15%), a time-dependent K$^+$ outward rectifier was observed. The close relationship between the reversal potential (E_{rev}) and the electrochemical equilibrium for K$^+$ (E_K^+) in the different bathing solutions indicated that K$^+$ was the main ion carrying these currents (Table I). The time-dependent K$^+$ currents showed whole-cell activation kinetics and K$^+$ selectivity similar to those characterized in protoplasts derived from mature root tissues from maize (Roberts and Tester, 1995) and other species (Schachtman et al., 1991; Findlay et al., 1994; Gassmann and Schroeder 1994; White and Lemtiri-Chlieh, 1995).

The fact that these currents co-existed (Fig. 1A) or occurred alone (Fig. 1B) in different cells, plus the fact that in some cells there was a lack of inward currents at membrane potentials negative of E_K^+, suggests that the three different K$^+$ currents are mediated by three different populations of channels. These three types of currents were suppressed when the intracellular and/or extracellular media contained tetraethylammonium (TEA; data not shown).

pH and Al^{3+} Effects on K$^+$ Whole-Cell and Single-Channel Conductances

Given the physical chemistry of Al (i.e. Al^{3+} is the predominant and toxic Al species at low pH values), we proceeded to dissect and characterize plasma membrane transport under Al^{3+}-toxic conditions. We first evaluated the effect of imposing an extracellular acidic environment on ion transport. Extracellular acidification had two major effects on the predominant K$^+$ currents (Fig. 1C). First, it stimulated the inward time-dependent K$^+$ current. The current recorded at pH 4 was between 2 and 4 times larger than that recorded at pH 6 with the stimulation being larger as the holding potential became more nega-
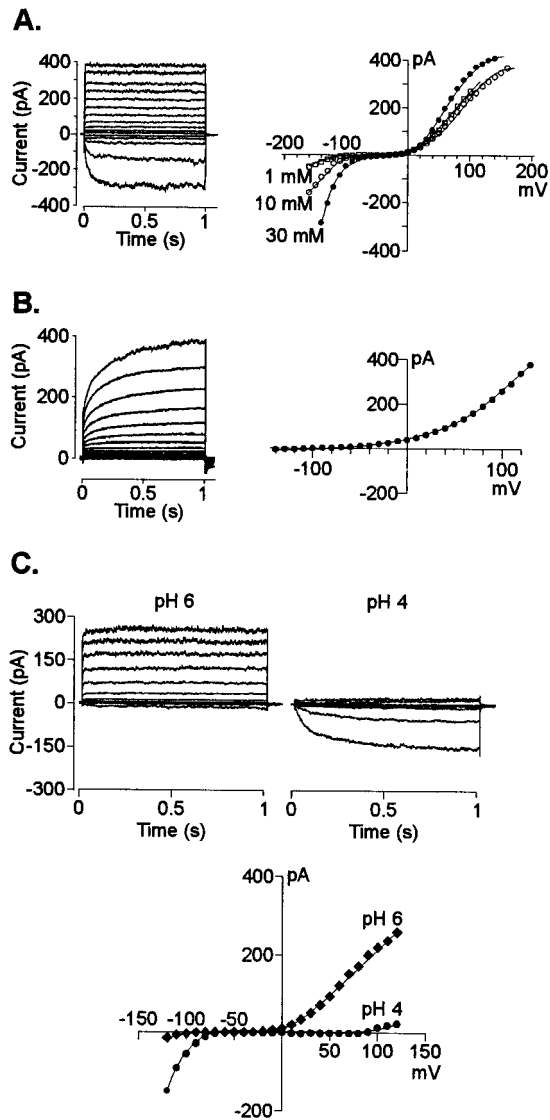
Figure 1. Example of the whole-cell K^{+} currents and their respective current-voltage (I/V) relationships, measured across the plasma membrane of maize protoplasts isolated from the first 5 mm of the root. The patch pipette contained K^{+}-based filling solution (see "Materials and Methods" for the detailed explanation on voltage protocols). For clarity, only currents in response to 20 mV steps are shown. A, Instantaneous outward and time-dependent inward K^{+} currents recorded from a cell with a diameter of 35 μm and bathed in a solution containing 10 mM K^{+} (pH 6). Right, I/V relationships from the currents shown on the left in bath solutions containing 10 (○) as well as 1 (□) and 30 mM (●) K^{+} (pH 6). Similar results for K^{+} selectivity were obtained in nine other cells. B, Time-dependent outward K^{+} currents and their respective I/V relationship (right) recorded in a cell with a diameter of 28 μm bathed in a solution containing 1 mM K^{+} (pH 6). C, Effect of extracellular pH on the instantaneous outward and time-dependent inward K^{+} currents from a 36-μm diameter cell bathed in a solution containing 10 mM K^{+} at either pH 6 or 4. The I/V relationships for the currents obtained at pH 4 (●) and pH 6 (♦) are shown on the right. The effect of pH on the currents was reversible upon restoring the original pH in the bath medium. Similar observations were recorded in four other cells.

tive. In contrast, extracellular acidification caused a dramatic inhibition of the instantaneous outward currents. The currents recorded at pH 4 were between 5 and 12 times smaller than that recorded in pH 6 with the degree of inhibition being larger at less positive holding potentials. The magnitude of the current inhibition was larger as the pH of the extracellular medium was progressively reduced from pH 7 to 4 in 1-pH-unit changes (data not shown). The remaining outward current recorded at pH 4 was further inhibited by perfusing the bath with a solution containing TEA, a K^{+} channel blocker. The pH effects on the inward and outward currents were observed in cells in which both types of currents co-existed (as shown in the figure), and in cells in which only one of the currents dominated the whole-cell conductance. In contrast, the time-dependent K^{+} outward rectifier seen in a small fraction of the cells was relatively insensitive to changes in extracellular pH (data not shown).

These results established which currents were likely to dominate the whole-cell conductance in an acidic extracellular environment. Consequently, we proceeded to evaluate the additional effect of extracellular Al^{3+} at low pH on root cell ion transport processes. The activity of Al^{3+} added to the bath solutions was similar to that previously found to simultaneously trigger a large organic acid (citrate) release in the maize genotype used in the present work and elicit the maximal difference in Al tolerance (measured as inhibition of root growth) between this and Al-sensitive maize genotypes (Pellet et al., 1995). Addition of 50 μM Al (Al^{3+} activity = 12 μM) significantly inhibited (80%–90% inhibition) the remaining instantaneous outward K^{+} conductance (i.e. already inhibited by the low extracellular pH) (Fig. 2). Extracellular Al^{3+} also inhibited the time-dependent K^{+} inward rectifier (Fig. 3). The inhibition was both concentration and voltage-dependent with the magnitude of the inhibition being larger as the holding potentials became more negative. The sensitivity of the inward rectifier to Al^{3+} was less than that observed

The pipette solution contained either KCl (K-based) or TEA-Cl (TEA-based). Equilibrium potentials were determined from the ionic activities calculated using the GEOCHEM-PC speciation program. Values are given in mV. The equilibrium potential for Mg^{2+} (not shown) was set at very negative potentials ($\gg-$) in all cases.

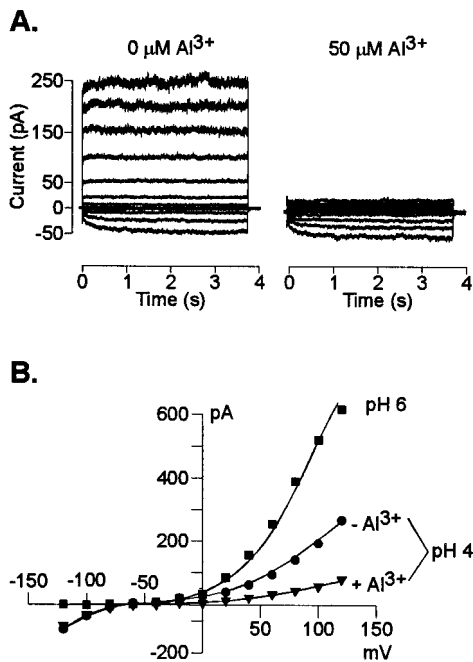| Pipette	Bath	E_{Cl^-}	E_{K^+}	E_{TEA^+}	$E_{Ca^{2+}}$
K-based	1 K^{+}	94	−111	−	113
K-based	10 K^{+}	53	−54	−	113
K-based	30 K^{+}	29	−27	−	113
TEA-based	Sealing	30	$\gg+$	$\gg-$	146
TEA-based	1 TEA	94	−	−111	113
TEA-based	10 TEA	56	−	−54	113
TEA-based	150 TEA	−9	−	11	113

A.

B.

Figure 2. Blockade of the instantaneous outward K$^+$ current by extracellular Al^{3+}. The pipette contained K$^+$-based solution. A, Currents recorded from a 32-μm-diameter cell bathed in 10 mM K$^+$ (pH 4; left) and subsequently perfused with the same bath solution containing 50 μM Al^{3+} (right). B, I/V relationship of the currents shown in A recorded in bath solutions (pH 4) lacking (●) and containing (▼) Al^{3+}; the I/V relationship obtained in 10 mM K$^+$ (pH 6) is shown for reference (■). Similar observations were recorded in a total of six cells under identical ionic regimens.

for the instantaneous outward current with the current being inhibited only between 22% to 32% by 50 μM Al. Elevating extracellular Al to concentrations as high as 400 μM only inhibited this current by 46% (at a holding potential of -120 mV). In an effort to further characterize these inhibitory effects, we also examined the effect of extracellular Al^{3+} on single K$^+$ channel properties. In the absence of Al^{3+}, we could regularly (10 of 18 excised patches) detect the single activity of one type of K$^+$ outward channel. This channel had a unitary conductance of 15 ± 2 pS (in 10 mM K$^+$) in both pH-6 and -4 solutions. Addition of extracellular Al^{3+} blocked the single-channel K$^+$ currents (Fig. 4). The blockade appeared to be fast with the time transitions of the blocking and unblocking reactions being too fast to be resolved at the cutoff frequency of the filtering used and thus appearing as a time-averaged reduction in the single-channel current amplitude. The single-channel blockade by extracellular Al^{3+} was also concentration and voltage dependent with the current inhibition being greater at more negative holding potentials. This observation suggests a direct effect of the voltage on the association/dissociation rates of Al^{3+} binding to a site within the channel. However, in contrast to the high affinity blockade of the outward current in whole cells, 50 μM Al caused only a 7% reduction of the

unitary conductance at the single-channel level (with no significant change in the reversal potential). Increasing Al^{3+} concentrations to as high as 330 μM resulted in further inhibition of the single-channel unitary conductance, but only to approximately a 28% reduction of the unitary conductance recorded in the control.

Al^{3+} Induces Whole-Cell and Single-Channel Anion Currents in Protoplasts Isolated from the Root Apex

The above results indicated that K$^+$ conductances could still be detected in whole-cell and isolated patches at low extracellular pH and even in the presence of large extracellular Al^{3+} activities. Thus, we proceeded to replace the K$^+$ in the intracellular and/or bath solutions with TEA to suppress the background K$^+$ currents and facilitate dissection of other less predominant currents. A total of 39 cells were examined under these experimental ionic conditions. We occasionally ($n = 5$) recorded one type of single anion channel activity in excised outside-out patches (Fig. 5). The kinetics of the channel were
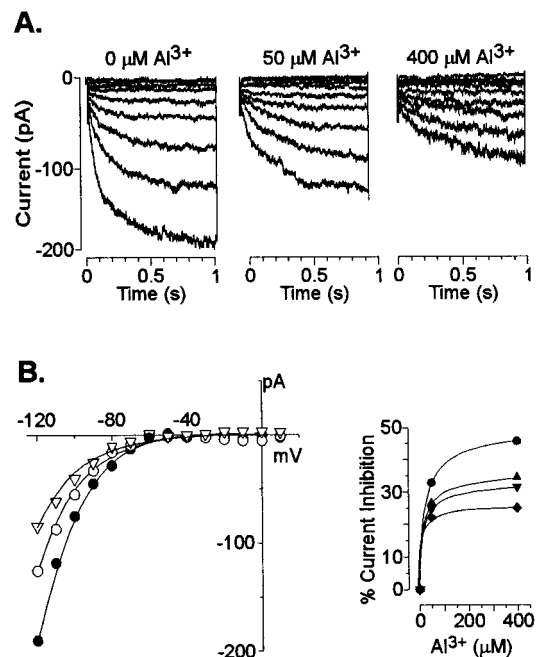
A.

B.

Figure 3. Blockade of the whole-cell time-dependent inward K$^+$ currents by extracellular Al^{3+}. A, Currents were recorded in a 36-μm-diameter cell and bathed in 10 mM K$^+$ (pH 4), which was then perfused with the same solution containing different levels of Al^{3+} as described at the top of each set of traces. The pipette contained K$^+$-based solution. B, The I/V relationship (left) for the currents shown in A recorded in solutions lacking (●) or containing 50 μM (○) or 400 μM (▽) Al^{3+}. Current inhibition (right) as a function of extracellular Al^{3+}. The percentage of current inhibition was calculated from the ratio of the current magnitude in the presence and absence of Al^{3+} at potentials of -118 (●), -108 (▲), -98 (▼), and -88 (◆) mV. Data points are from one representative experiment. Similar observations were recorded in a total of four cells.
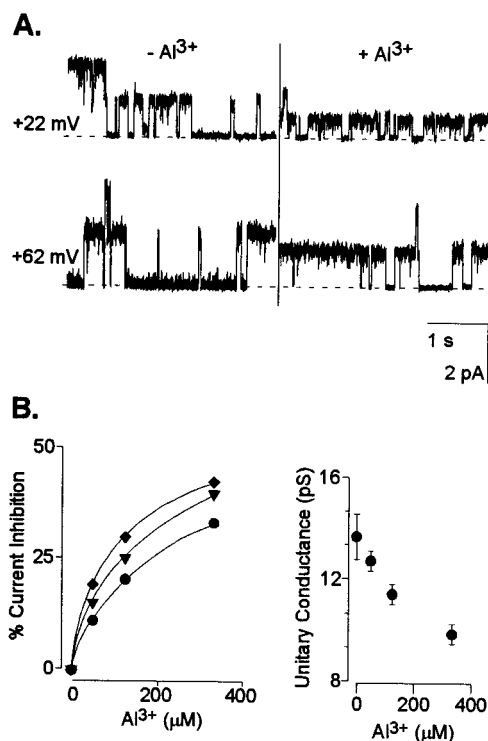
A.

B.

Figure 4. Effect of extracellular Al^{3+} on the amplitude of K^+ single-channel currents. A, Single-channel recordings from an outside-out patch with a K^+-based filling solution and bathed in 10 mM K^+ (pH 4) solution $\pm$ Al^{3+}. The traces shown were recorded at the holding potential indicated in the left margin in the absence and presence of 330 μM Al^{3+}. The horizontal dashed line represents the closed state. B, Single-channel current inhibition as a function of extracellular Al^{3+}. Left, The percentage of current inhibition was defined as the ratio of the recorded currents in the presence and absence of varying Al^{3+} concentrations at test potentials of +82 (●), +62 (▼), and +22 (◆) mV. Right, Single-channel unitary conductance inhibition as a function of extracellular Al^{3+}. The unitary conductance values were calculated as described in "Materials and Methods" (r^2 values ranged between 0.988 and 0.998). There were no significant differences in E_{rev} among treatments. Similar observations were recorded in a total of four different patches.

distinct, displaying long opening and closing times, in the range of seconds. The channel activity did not "rundown" over time, even 1 h after excising the patch. This channel had a small inward and outward unitary conductance (approximately 2–4 pS) in 11 mM extracellular Cl^- and consequently has been designated as SCAC (small conductance anion channel). The unitary conductance of the outward current carried by SCAC increased to 9.2 $\pm$ 0.5 pS when the Cl^- activity was increased to 115 mM Cl^-. The I/V relationship constructed from steady-state recordings as well as those derived from slow voltage ramps established that the currents reversed near and followed changes in equilibrium for Cl^- (E_{Cl^-}; Table I). This indicated that among all ions present in the intracellular and bath solutions, the current across the channel was carried by Cl^- (Fig. 5, B and C). This channel was able to mediate both anion efflux (in-

ward currents) as well as anion influx (outward current). Reconstruction of macroscopic inward currents from this channel showed that at depolarizing membrane potentials (more negative than E_{Cl^-}) the channel was able to sustain anion efflux, undergoing only a very slight inactivation over time (Fig. 5D).

Whole-cell recordings established that replacement of intracellular and/or extracellular K^+ by TEA greatly reduced the whole-cell conductances. The lack of large inward anion currents in isolated patches in the presence of TEA correlated with the detection of small inward currents in whole-cell measurements where cells were exposed to similar ionic conditions. With TEA-based solutions in the pipette and 1 mM TEA (pH 4) in the bath, small currents (presumably mediated by SCAC) dominated the whole-cell conductance and reversed at 56 $\pm$ 3 mV ($n = 12$ cells), close to E_{Cl^-} (Fig. 6). Under these ionic conditions, addition of extracellular Al^{3+} caused an immediate shift in E_{rev} to more a positive membrane potential (97 $\pm$ 4 mV; $n = 10$ cells), with the magnitude of the shift averaging 41 $\pm$ 2 mV (Fig. 6). This shift suggests Al^{3+}-activation of an inward current, which was verified by the observation that in 40% of the cells examined, the shift in E_{rev} was accompanied by the activation of a small (compared with the large K^+ conductances described above) inward current (Fig. 6A). This whole-cell current was activated within minutes following perfusion of the bath solutions with extracellular Al^{3+}. At negative holding potentials, this Al^{3+}-induced current activated instantaneously and then partially deactivated with time. The remaining activated current (measured at steady state) was 30% to 50% of the current magnitude measured within 100 ms of imposition of the test potential.

The Al^{3+}-activated current reversed at holding potentials near the theoretical reversal potential for Cl^-, suggesting this inward current was being selectively carried by Cl^-. The activation of this current by extracellular Al^{3+} was occasionally (25% of the total cells where activation was observed) detected as an activation of individual single-channel events in the whole-cell configuration (Fig. 6B). Take together, these observations indicated a low density of this particular Al^{3+}-activated channel. Single-channel events in whole-cell configuration allowed a more accurate estimate of E_{rev} (+96 mV), confirming the close relationship between the reversal potential of the current and the theoretical reversal for Cl^- (see I/V relationship in Fig. 6B). In addition, the unitary conductance of this channel was significantly larger than that recorded for SCAC, and this channel was active only in the presence of Al^{3+}. We have designated this Al^{3+}-activated channel as LCAC (large conductance anion channel). Under the electrical conventions used in the present work, these Al^{3+}-activated inward currents correspond to Cl^- efflux. Similar Al^{3+}-activated currents were recorded in
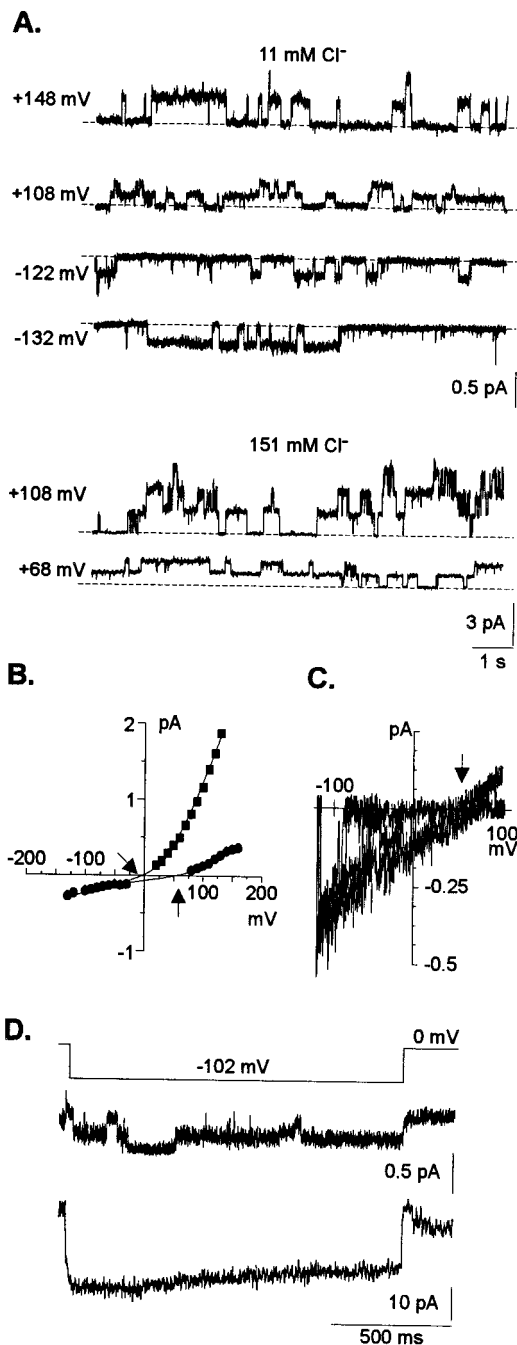
Figure 5. Single-channel recordings of SCAC from outside-out patches in the absence of Al³⁺. The pipette solution was TEA-based. All traces were taken from one representative experiment. Recordings containing a single anion channel activity similar to the one described above were obtained from five different excised patches. The time and current scales for the individual and for the summed recordings are given on the bottom right side of each set of traces. See "Materials and Methods" for voltage protocols, calculations, and data transformations. A, Example of single anion channel activity at two different extracellular Cl⁻ concentrations as indicated on the top of each set of traces. Membrane potentials were stepped from 0 mV to the voltage indicated in the left margin. Given the small conductance of the channel, currents were filtered at 200 Hz. Note the different current scales for each ionic condition. The horizontal dashed lines represent the closed state. B, I/V relationship for single

cells where the pipette contained K⁺ based solutions, providing that the K⁺ background currents prior to Al³⁺ exposure were small enough to allow us to resolve the small inward currents activated after Al³⁺ exposure (data not shown).

Further characterization of the permeability and selectivity of LCAC was performed in outside-out patches isolated from protoplasts that had been exposed to Al³⁺ prior to patch excision. LCAC was readily (7 of 16 patches) recorded in bath solutions containing Al³⁺ (Fig. 7A). In contrast to SCAC, this second type of channel was only recorded in patches exposed to Al³⁺ and had different kinetics and unitary conductance. LCAC exhibited a characteristic "noisy" open state, and its unitary conductance was significantly larger than that of SCAC. The unitary conductance of LCAC ranged from 18 to 27 pS, increasing as the extracellular Cl⁻ concentration in the bath increased (Fig. 7, B and C). The unitary conductance values were in the range of those commonly reported for other plant anion channels (approximately 10–40 pS; although unitary conductances as large as 150 pS have also been reported [Terry et al., 1991; Amtmann et al., 1997]). Similar kinetics and unitary conductance values for this Al³⁺ activated channel in excised patches were observed when the pipette solution contained K⁺ and the bath solution contained KCl and extracellular Al³⁺ (Fig. 7D). The I/V relationships derived from slow voltage ramps indicated the single-channel current reversed at holding potentials close to the electrochemical E_{Cl^-}. Increasing the Cl⁻ concentration in the bath solution caused a negative shift in the E_{rev} of the single-channel current, closely following the change in E_{Cl^-} (Fig. 7, B and C). These observations indicated that for the ions present in the pipette solution (in both K⁺ and TEA-based filling solutions), the inward current was being selectively carried by Cl⁻. Thus, the data from isolated patches in Figure 7 provided further support for the anion selectivity of the Al³⁺-induced inward current that was previously inferred from macroscopic and single-channel currents observed in whole-cell preparations.

-channel recordings when the bath solution contained 11 (●) or 151 (■) mM extracellular Cl⁻. The right and left arrows indicate the theoretical reversal potential for Cl⁻ when the bath contained 11 or 115 mM Cl⁻, respectively. In 11 mM Cl⁻ the unitary conductances and E_{rev} were 1.6 ± 0.1 pS and +33.9 mV (r^2 = 0.943) for the inward current and 4.2 ± 0.2 pS and +66 mV (r^2 = 0.971) for the outward current, respectively. In 115 mM Cl⁻ the unitary conductance of the outward current was 9.2 ± 0.5 pS and the E_{rev} was +7.6 mV (r^2 = 0.992). C, I/V relationship derived from slow voltage ramps from an outside-out patch with 11 mM Cl⁻ in the bath solution The arrow indicates the theoretical reversal potential for Cl⁻. The unitary conductance of the inward current was 2.5 pS. D, Reconstruction of macroscopic current (second trace) from the single-channel activity (first trace) elicited by the voltage protocol shown on top of the trace.
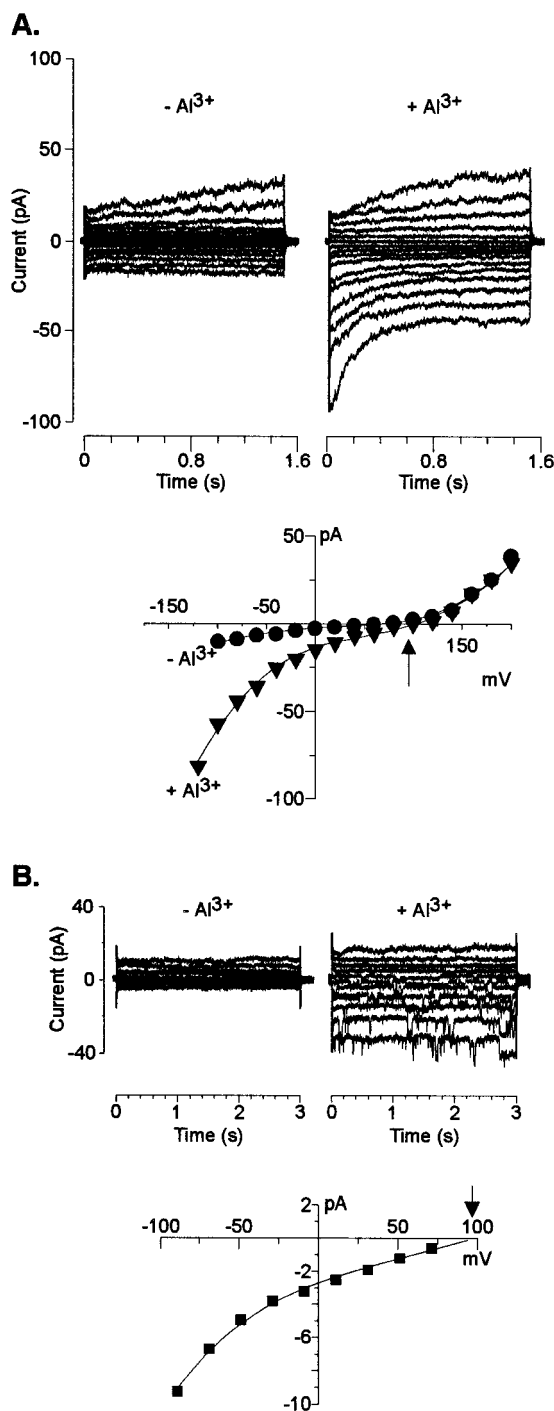
A.

B.

Figure 6. Al^{3+}-induced inward anion current. The pipette solution for the two cells shown in these examples was TEA-based and the recordings were obtained in 1 mM TEA-Cl (pH 4) in the absence and presence of 50 μM extracellular Al^{3+} (12 μM activity), following a voltage protocol as described in "Materials and Methods." The arrows indicate the theoretical reversal potential for Cl^-. A, Whole-cell recordings obtained from a 32-μm-diameter cell. The I/V relationship from these traces was constructed by measuring the magnitude of the outward currents at the end of the voltage pulse, whereas the current magnitude of the instantaneous inward currents were measured 100 ms after imposition of the test pulse. Similar whole-cell recordings were obtained in total of 12 cells. B, Single-channel events induced

Single-Channel Characterization of the Mechanism of Al^{3+} Activation

Figure 8A shows a representative example of a patch excised in the presence of extracellular Al^{3+}, where the activity of the two types of anion channels described previously (LCAC and SCAC) were recorded. It is worth highlighting that LCAC was only observed in excised patches that were exposed to extracellular Al^{3+}, whereas SCAC (i.e. the SCAC described in Fig. 5) was observed in excised patches in the presence and absence of extracellular Al^{3+}. This observation suggests that the activity of LCAC was dependent on the presence of extracellular Al^{3+}. Figure 8B shows a recording illustrating the requirement of extracellular Al^{3+} to maintain the activity LCAC. Single-channel activity was detected in a patch excised from a cell that was exposed to extracellular Al^{3+}. Under these conditions, the channel remained active as evidenced by the frequent opening and closing events over a time scale of minutes. Upon removal of Al^{3+} from the bath, the channel inactivated and remained in its closed state. This process was reversible (i.e. channel re-activation) by re-introducing Al^{3+} to the bath solution (data not shown). The specificity of the response was also confirmed by the fact that exposure to equivalent extracellular La^{3+} concentrations in the absence of extracellular Al^{3+} did not restore channel activity (data not shown).

Having established the dependence on Al^{3+} for activation of LCAC, the following experiments were conducted to isolate and delimit the mechanism and pathways involved in the processes of channel activation by Al^{3+}. For such purposes we attempted to trigger channel activation in excised patches (Fig. 9). We selected "electrically quiet"(i.e. lacked any channel activity) outside-out patches excised from protoplasts that had not previously been exposed to extracellular Al^{3+}. Lack of channel activity was confirmed by voltage protocols in which no channel activity was evoked in any of the 60 repetitions performed, as illustrated by the thin (i.e. quiet) closed state (Fig. 9B). When the "quiet" patches were exposed to extracellular Al^{3+}, a channel mediating an inward current (downward deflection) was activated (Fig. 9C). Channel activity in the presence of Al^{3+} was sustained, as indicated by a thick continuous open state, which was the product of superimposing traces containing a large number of opening and closing events over the 60 repetitions of the voltage protocol. Re-

A.

-42 mV

-52 mV

-82 mV

-102 mV

1 s

2.5 pA

B.

2 pA

-100

100 mV

-4

-6

1 mM TEA

C.

2 pA

-100

100 mV

-4

-6

10 mM TEA
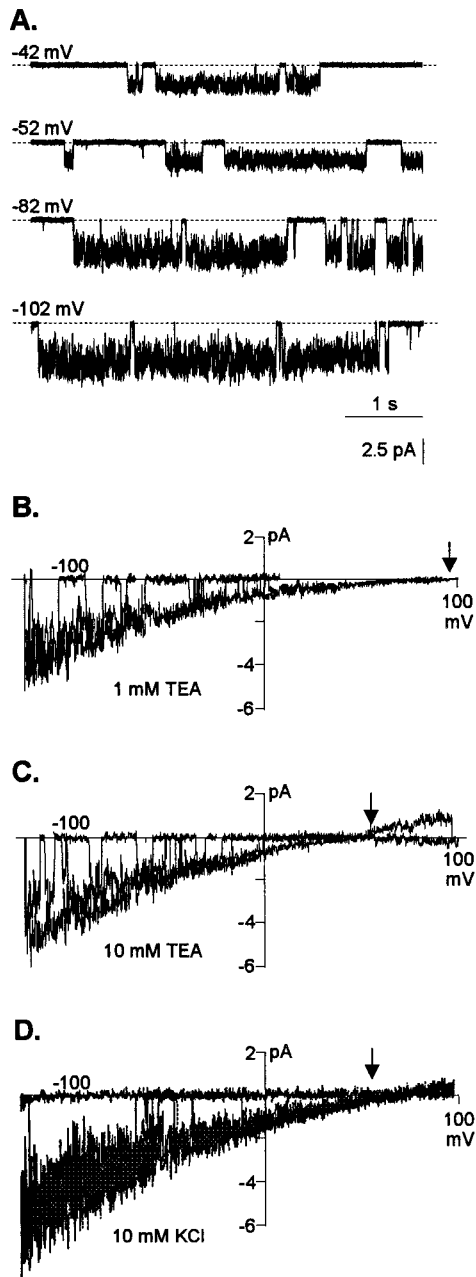
D.

2 pA

-100

100 mV

-4

-6

10 mM KCl

Figure 7. Ion selectivity of the LCAC activated by the presence of Al³⁺. A, Examples of single-channel recordings from outside-out patches. The pipette solution was TEA-based and the bath solution contained 50 μM AlCl$_3$ in 10 mM TEA-Cl (pH 4.0). Membrane potentials were stepped from 0 mV to the voltage indicated in the top left margin of each trace. The horizontal dashed lines represent the closed state. B to D, Current-voltage (I/V) relationships derived from slow voltage ramps (see "Materials and Methods"). The arrows indicate the Cl⁻ theoretical reversal potential for each ionic condition. The pipette solution was TEA-based and the bath solution contained 50 μM AlCl$_3$ in 1 mM TEA-Cl (pH 4.0) (B) or 10 mM TEA-Cl (pH 4.0) (C). The unitary conductances under these conditions were 18 and 27 pS, respectively. Similar results were obtained with other cells when the pipette solution was K⁺-based and the bath solution contained 50 μM Al³⁺ in 10 mM KCl (D). In this case, the unitary conductance was 25 pS. Similar channel activity and selectivity was recorded in a total of seven different patches in the different ionic environments containing extracellular Al³⁺.

construction of macroscopic currents (Fig. 9D) for this particular channel shows that at depolarizing membrane potentials the channel is able to maintain sustained anion efflux, as it does not undergo inactivation, at least over the time periods tested under this voltage protocol (1.4 s). Upon removal of Al³⁺ from the bath solution, the channel once again inactivated (data not shown), in agreement with previous observations (i.e. Fig. 8B). These results indicated that the mechanism required for triggering channel activation is solely localized to the plasma membrane (i.e. a membrane bound response). That is, either the channel protein is directly activated when it binds Al³⁺ or the Al receptor and signal transduction pathways are localized to the plasma membrane in close proximity to the Al³⁺-activated channel (LCAC).

DISCUSSION

In this study, the patch-clamp approach was used to further our understanding of some of the ion transporters that are likely to be involved in Al-tolerance mechanisms that take place in root tip cells of Al-tolerant maize. Figure 10 summarizes the main observations recorded for some of these transporters upon extracellular acidification and/or exposure to extracellular Al³⁺.

LCAC. An Al³⁺-Activated Anion Channel

In this study the functioning of an Al³⁺-activated anion channel (designated as LCAC) was described. This channel has some similarities to an Al³⁺-activated channel reported from protoplasts isolated from the root apex of Al-tolerant wheat (Ryan et al., 1997). Our work extends and refines the understanding of Al-activation of this anion channel by providing evidence for Al-dependent channel regulation at the single-channel level. The Al dependence and Al activation of the channel in isolated patches represents a major breakthrough in our understanding, as it indicates that the mechanism for channel activation is solely localized to the plasma membrane (i.e. a membrane-bound response). That is, either the channel protein is directly activated when it binds Al³⁺, or the Al receptor and signal transduction pathway are limited to the plasma membrane and are co-localized with the channel. The lack of inactivation of LCAC at the single-channel level (i.e. in excised patches) suggests that the loss of cytoplasmic integrity (e.g. washout of cytoplasmic factors by the pipette solution) does not disrupt the mechanism(s) necessary to maintain this channel in the active state. Although our findings reported here establish that this channel can catalyze a Cl⁻-selective efflux, permeability and selectivity sequences derived from other studies have established that plant cell anion channels are permeable to a variety of inorganic and organic anions (Hedrich et al., 1990; Terry et al., 1991;
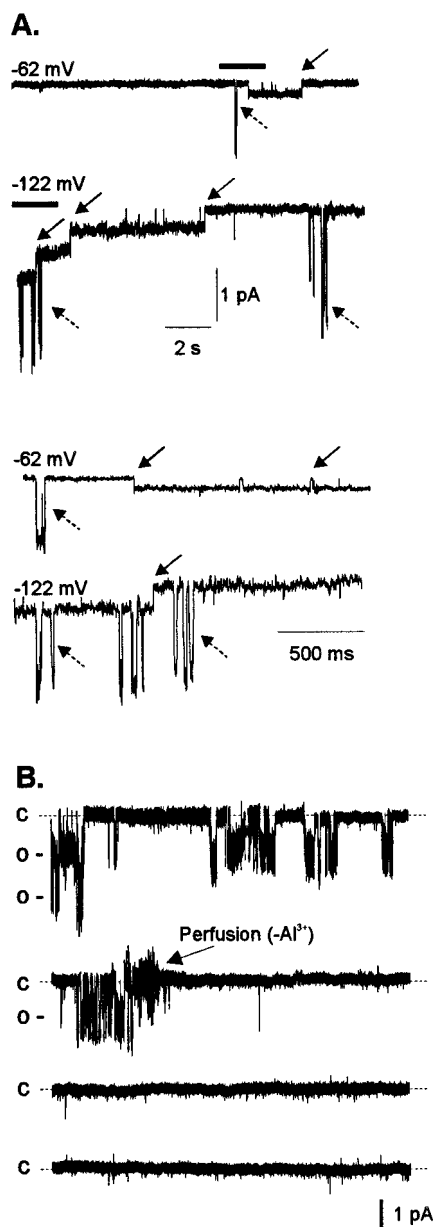
A.

B.

Iwasaki et al., 1992; Pantoja et al., 1992; Tyerman, 1992; Schmidt and Schroeder, 1994; Schroeder, 1995; Dietrich and Hedrich, 1998; Frachisse et al., 1999). In addition, the unitary conductance of LCAC in maize is also dependent on extracellular anion activities, an intrinsic channel property that has been proposed to enable the cell to sustain anion efflux, despite the reduction of the electrochemical gradient across the membrane as the extracellular anion concentration increases (Hedrich and Marten, 1993). Given these generalized selectivity and permeation properties, and taking into consideration the biophysical properties exhibited by LCAC, it is likely that LCAC mediates the Al-induced organic acid release observed in whole root studies (Pellet et al., 1995).

SCAC

This second type of anion channel, which was readily observed in excised patches bathed in solutions designed to minimize K^+ conductances (i.e. pipette and bath solutions containing TEA and lacking extracellular Al^{3+}), mediates both a selective influx and efflux of anions. Single-channel kinetics, as well as reconstructed macroscopic currents from single-channel recordings, indicated this channel was able to maintain a sustained anion efflux at potentials negative of E_{Cl^-} and exhibited a very slow inactivation with time. These kinetics resemble those described for the slowly activating anion conductance in root parenchyma cells (Wegner and Raschke, 1994; Köhler and Raschke, 2000) and the S-type channel in guard cells (Schroeder and Keller, 1992). Also, we found that SCAC also mediated a large outward current at very positive potentials (at low extracellular Cl^- concentrations), or at moderate positive membrane potentials under high extracellular Cl^- concentrations, resembling the anion outward rectifier in other plant cells (Terry et al., 1991; Skerrett and Tyerman, 1994; Köhler and Raschke, 2000). The existence SCAC and other additional types of plasma membrane anion channels may account for the low levels of Al^{3+}-independent organic acid release described previously in whole root studies.

Whole-Cell Anion Currents

Both maize (M.A. Piñeros and L.V. Kochian, unpublished data) and wheat (Ryan et al., 1995a) show very rapid (appearing to occur almost instantaneously after Al exposure) Al-induced root organic acid exudation, which is localized to the root apex. However, whereas malate is the only organic acid

Figure 8. Extracellular Al^{3+} is required for maintaining activity of LCAC. A, Examples of single-channel recordings from an outside-out patch containing the two types (i.e. LCAC and SCAC) of anion channels. Membrane potentials were stepped from 0 mV to the voltage indicated in the top left margin of each trace. Downward deflections indicate channel opening. The solid arrows indicate single-channel events for SCAC, the anion channel observed with and without Al^{3+}. The dashed arrows indicate single-channel events for LCAC, the anion channel observed only in solutions containing Al^{3+}. The pipette solution was TEA-based and the bath solution contained 50 μM Al^{3+} in 1 mM TEA-Cl (pH 4.0). For clarity, the section of each trace indicated by the thick horizontal line above it has been enlarged and presented in the bottom two traces of Figure 8A. B, Continuous 8-min single-channel trace (each trace containing 2 min of recording) from an outside-out excised patch containing two channels of LCAC, recorded at a holding potential of -39 mV. The pipette solution was K^+-based and initially the bath solution contained 1 mM TEA-Cl (pH 4.0) and 50 μM Al^{3+}. The arrow on the second trace indicates the time (2 min, 34 s) when the recording

chamber was perfused with an identical bath solution lacking Al^{3+}. Labels on the left of each trace represent the closed (C) and open (O) states of the channel. The current amplitude scale is shown at the right bottom of the Figure. Similar results were obtained in another excised patch.
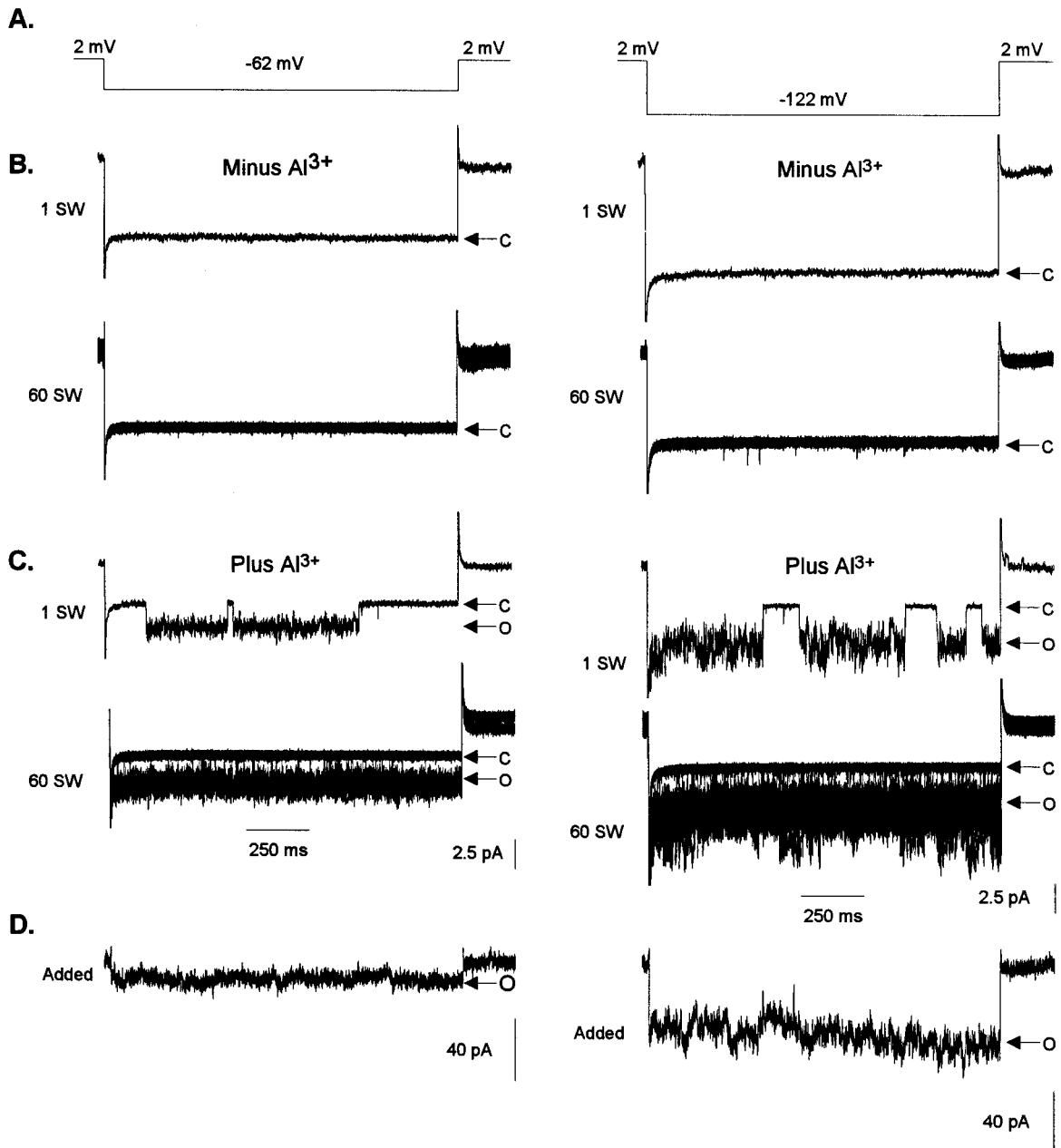
Figure 9. Extracellular Al³⁺ activates single channels in outside-out patches excised in the absence of Al³⁺. The pipette contained K⁺-based filling solution. Bath solutions contained 1 mM TEA-Cl (pH 4.0) plus or minus 50 μM Al³⁺. Arrows and labels on the right represent the closed (C) and open (O) states of the channel. The time and current scales for B and C are shown at the bottom of C. The current scale D is at the bottom; the time scale is the same as in B and C. A, Two voltage protocols were used to test for single-channel activity in solutions lacking and containing Al³⁺. The voltage was stepped from a holding potential of 2 mV to −62 (left column) or −122 mV (right column) and held at this test potential for 1.4 s before returning to the holding potential. B, Resulting trace of one single sweep (1 SW: one sweep) from the voltage protocol described in A. The protocol described in A was repeated consecutively 60 times with a 5-s resting phase between repetitions. The panel labeled 60 SW shows the 60 repetitions of individual sweeps superimposed. C, Same voltage protocol as in A after 50 μM Al³⁺ was added to the bath solution. As in B, 1 SW shows a trace for one of the 60 sweeps, and 60 SW shows the traces of all 60 sweeps superimposed. D, Reconstruction of macroscopic currents from the 60 single-channel sweeps shown in C (see "Materials and Methods" for a detailed description of reconstruction protocols). Similar results were obtained in a total of three different excised patches.

released in wheat, citrate is the primary organic released from maize roots. The differences between the Al³⁺-induced anion currents in maize and wheat root apical protoplasts (e.g. the current density and current kinetics) are likely to reflect differences observed at the whole root level (Delhaize et al., 1993a, 1993b;
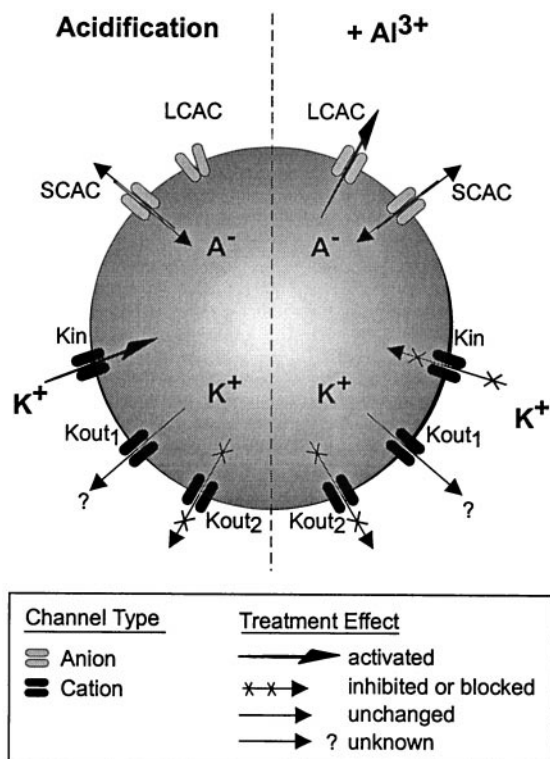
Figure 10. Summary of the alterations induced in plasma membrane ion transporters for root tip cells of Al-tolerant maize upon extracellular acidification or exposure to extracellular Al^{3+}. The channel nomenclature is as follows: LCAC corresponds to the Al^{3+}-activated LCAC; SCAC to the Al-independent SCAC; K_{in} to the K^+ inward rectifier; $K_{out}1$ to the time-dependent K^+ outward rectifier; and $K_{out}2$ to the K^+ instantaneous outward rectifier channel, respectively. Channel activation is indicated by an arrow of increased thickness, whereas channel inhibition or blockade is indicated by crosses superimposed on the arrows representing ion flux through a channel.

Ryan et al., 1995a; Pellet et al., 1995, 1996). In maize, this current exhibits characteristics previously described for the quick activated anion conductance and the S-type anion channels described in root parenchyma and in guard cells (Schroeder and Hagiwara, 1989; Hedrich et al., 1990; Schroeder and Keller, 1992; Köhler and Raschke, 2000). It is worth noting that the whole-cell anion currents recorded in maize in the presence of Al^{3+} are the sum of the activity of LCAC as well as SCAC channels. However, reconstructed macroscopic currents from SCAC and LCAC recordings indicate that these channels were able to mediate a sustained anion flux (i.e. showed no inactivation), in contrast to the partial inactivation of the Al^{3+}-induced inward currents observed in whole-cell preparations. Although the exact mechanisms and factors determining the partial inactivation recorded in the whole-cell configuration remain unknown, these differences suggest some likely scenarios. A complex cascade of events regulating this channel might be involved, such that in addition to the requirement of extracellular Al^{3+} for channel activation, other intracellular and extracellu-

lar factors may modulate the activity of this channel in the whole-cell mode. The activity of other voltage gated plant anion channels have been shown to be modulated by a wide range of signals such as changes in intracellular and/or extracellular Ca^{2+} and anion activities as well as protein phosphorylation or allosteric regulation by nucleotides (Schroeder and Hagiwara, 1989; Hedrich et al., 1990; Skerrett and Tyerman, 1994; Zimmermann et al., 1994; Schmidt et al., 1995; Thomine et al., 1995, 1997; Schulz-Lessdorf et al., 1996; Tyerman et al., 1997; Frachisse et al., 1999). Although similar processes could underlie the difference between the macroscopic currents and the single-channel recordings reported here, contributions by other type(s) of anion channel(s) activated by Al^{3+} cannot be ruled out.

pH and Al^{3+} Effects on K^+ Channels

Under physiological conditions (K^+ in the bath and pipette), instantaneous K^+ outward currents dominated the whole-cell conductance in root tip cells in maize, although occasionally a time-dependent K^+ inward rectifier and/or a time-dependent K^+ outward rectifier were also recorded. As work on Al tolerance requires that the studies be conducted at acidic extracellular pH, it was interesting to note that extracellular acidification stimulated the time-dependent K^+ inward rectifier. It was presumed that the mechanisms underlying the stimulation of this current in maize root cells are similar to that recently reported for inward K^+ channels in root cells (Amtmann et al., 1999). In contrast, although the whole-cell instantaneous K^+ outward current in maize root tip cells was gradually inhibited as the pH of the extracellular medium was decreased, the unitary conductance of single channels mediating the K^+ outward currents remained unchanged at different extracellular pH values. It was presumed that pH regulation of this current is due to a changes in the local electrical field sensed by the gating structures of the channel, similar to that proposed for the time-dependent K^+ outward current from guard cells (Ilan et al., 1994).

The addition of Al^{3+} had different effects on the inward and outward K^+ currents. Although high affinity blockade (one-half maximal inhibitions occurring at Al^{3+} activities of approximately 10 μM) by extracellular Al^{3+} has been previously reported for K^+ inward currents (Gassmann and Schroeder, 1994; Ryan et al., 1997) and Ca^{2+} inward currents (Piñeros and Tester, 1995, 1997) from wheat root cells, the K^+ inward current observed in the present study showed little or no inhibition at similar extracellular Al^{3+} activities (12 μM Al^{3+} activity; total Al concentration of 50 μM). This current was moderately inhibited in a voltage-dependent manner as the extracellular Al concentration increased to 400 μM (128 μM Al^{3+} activity). In contrast, exposure to 12 μM Al^{3+}

activity almost completely inhibited the instantaneous K$^+$ outward current. Although the single-channel recordings for the K$^+$ outward current indicated that the binding of Al^{3+} within the channel pore disrupts the movement of the main permeant ion (K$^+$) along the conduction pathway, discrepancies in Al^{3+} sensitivity between the whole-cell and single-channel recordings indicate an additional effect of Al^{3+} on the activation and inactivation processes governing the whole-cell currents in maize.

Although the present study suggests that the Al^{3+}-activated anion channel is the underlying mechanism for the Al-triggered organic acid release in intact roots, the basis of the difference in this physiological response between Al-tolerant and -sensitive maize varieties remains unknown. If indeed this Al^{3+}-activated channel is the basis for Al tolerance, we currently can only speculate about the possible scenarios accounting for the differences observed in the whole root studies. For example, the Al^{3+}-activated channel may exist only in cells from the root apex of the tolerant varieties, or alternatively it may be present in both varieties but at different densities. Comparative studies between cells from the mature and the root tip regions isolated from both Al-tolerant and Al-sensitive varieties are planned for the future and will help establish the role of this particular transporter in conferring Al tolerance in maize.

MATERIALS AND METHODS

Plant Material and Protoplast Isolation

Seeds of maize (*Zea mays* hybrid South American 3) were surface sterilized in 0.5% (v/v) NaOCl for 15 min and then germinated in the dark for 2 d on filter paper saturated with deionized water. Germinated seeds were transferred to polyethylene cups with mesh bottoms, covered with black polyethylene beads, and then placed into the precut holes of the cover of a black polyethylene container that held 2.4 L of aerated 0.2 mM CaCl$_2$ solution. Seeds were grown for an additional 3 d (14-h-light/10-h-dark cycle at 22°C) before being used for protoplast isolation. Protoplasts were isolated from root tips using conventional enzymatic digestion and Suc gradient protocols. The first 5 mm of the primary root were finely chopped in 10 mL of a solution consisting of 500 mM sorbitol, 1 mM CaCl$_2$, 5 mM MES [2-(N-morpholino)ethanesulfonic acid]-KOH, pH 6.0, 0.5% (w/v) polyvinyl pyrrolidine (10,000 M_r), 0.5% (w/v) bovine serum albumin, 0.8% (w/v) cellulysin (Calbiochem-Novabiochem, La Jolla, CA), and 0.08% (w/v) pectolyase (Sigma, St. Louis). Following the incubation time (4 h at 30°C in a rotatory shaker), released protoplasts were purified using Suc step gradients as described by Schachtman et al. (1991).

Recording Solutions

All solutions were filtered (0.22-μm pore, Millipore, Bedford, MA) before use. Two types of intracellular solutions were used to fill the patch pipettes. These solutions contained 2 mM MgCl$_2$, 10 mM HEPES (N-2-hydroxyethyl-piperazine-N'-2-ethanesulfonic acid)-Tris, pH 7.2, 4 mM Na$_2$ATP, 2 mM EGTA, and 100 mM either KCl (K$^+$-based filling solution) or tetraethylammonium chloride (TEA-based filling solution). The free Ca^{2+} concentration in these solutions, as estimated by GEOCHEM, was 50 nM. Pipette filling solutions were adjusted to 720 mosmol kg^{-1} using sorbitol. The extracellular sealing solution contained 10 mM KCl, 10 mM CaCl$_2$, and 10 mM MES-TRIS, pH 6.0. Bath solutions used for recordings contained 0.5 mM CaCl$_2$ and either KCl or TEA-Cl at the concentration indicated for each particular experiment. The pH of these solutions was adjusted to 6 with 10 mM MES-TRIS or to 4 with 10 mM HCl. All bath recording solutions were adjusted to 700 mosmol kg^{-1} using sorbitol. Al^{3+} was added from a stock solution of 10 mM AlCl$_3$ made up in 10 mM HCl.

Electrophysiology

Patch-Clamp Technique

Whole-cell and single-channel currents from protoplasts were recorded at room temperature (22°C) with an Axo-patch 200A amplifier (Axon Instruments, Foster City, CA), using conventional patch-clamp techniques (Hamill et al., 1981). A single junction reference electrode (model MI-401F; Microelectrodes, Londonderry, NH) was connected to the reference input of the head stage. Electrodes were pulled from borosilicate glass capillaries (1.5-mm diameter without filament, catalog no. PG 52150–4, World Precision Instruments, Sarasota, FL) using a two-stage model P-87 Flaming-Brown horizontal electrode puller (Sutter Instrument, Novato, CA). Electrodes were coated with Sylgard (Dow Corning) and were fire polished using a CPM-2 microforge (Scientific Instruments, Westbury, NY). Electrodes for whole-cell recordings had a resistance of 5 to 8 MΩ (in sealing solution and with KCl pipette filling solution). Electrodes used for excised patch recordings had a resistance of 8 to 12 MΩ. The small chamber volume (less than 0.5 mL) allowed for rapid solution exchange. After giga-ohm seals were formed, gentle suction was applied to the interior of the pipette to obtain the whole-cell configuration. The cell cytoplasm and pipette solutions were allowed to exchange for 10 min prior to data recording. Cell integrity was monitored using a video camera (AVC-D7, Sony, Tokyo) attached to the microscope. Current recordings were performed in the absence of microscope illumination. Whole-cell series resistance and capacitance were partially compensated for by the amplifier. Liquid junction potentials were corrected as described by Neher (1992). The access resistance was usually less than 10 MΩ. Whole-cell and single-channel data were generally low-pass filtered at 1 kHz using the low-pass Bessel filter of the amplifier and digitized at 10 kHz, unless otherwise specified in the figure legends. Unfiltered single-channel data simultaneously were recorded and stored on videotape using a digital data recorder (VR-10B, Instrutech, Elmont, NY). Ionic activities were calculated using CHEOCHEM-PC

(Parker et al., 1995). The Nernst potentials for ions in the pipette and bath solutions are summarized in Table I.

Whole-Cell Voltage Protocols

Voltage protocols, current recordings, data storage, as well as data analysis were done with the software package PClamp 7 (Axon Instruments) and a Pentium II personal computer. In experiments where the pipette contained K^+ based solutions (see above) the voltage was clamped at a potential equal to the calculated E_K^+ value (Table I), and a sequence of step voltage pulses was applied with voltages ranging from -158 to $+162$ mV (in 10- or 20-mV increments). In experiments where the pipette contained TEA^+-based solution, the holding potential was set to 0 mV and voltage pulses stepped between -102 to $+198$ mV (in 20-mV increments). In either case, there was a 3-s resting phase at the holding potential between each voltage pulse. Current magnitudes were calculated after subtraction of the linear "leak" current as described by Roberts and Tester (1995). The current-voltage (I/V) relationships were constructed by measuring the current amplitude at the end of the test pulses (i.e. steady state).

Single-Channel Voltage Protocols

Single-channel current amplitudes for constructing I/V relationships were determined from Gaussian fittings of current-frequency distributions, using the Simplex and Levenberg-Marquardt least-squares methods. Unitary conductances and observed reversal potential (E_{rev}) were calculated from the linear regression of the linear portion of the I/V relationship (r^2 values are given in parenthesis). In experiments where the pipette contained TEA^+-based solution, I/V relationships were also derived from slow voltage ramps with outside-out patches. Slow voltage ramps (1.0–1.4 s each) were applied between -122 and $+118$ mV from a holding potential of 0 mV. Between each voltage ramp there was a 10-s resting phase at the holding potential. The I/V relationships were reconstructed by subtracting averaged ramps where no channel activity was observed from individual ramps where channel events were detected. The I/V relationships shown in each case contain at least 8 to 12 individual superimposed ramps showing the open and close states of the channel. The unitary conductance of the single channel from I/V relationships derived from ramp protocols was estimated from the slope of the linear portion of the open state of the channel. Reconstruction of macroscopic currents from single-channel recordings was done as follows: single-channel activity was elicited by stepping the membrane potential from 0 mV to a given test potential. This protocol was repeated 50 times, allowing a 5-s resting phase between repetitions. Capacitative currents were removed by subtracting a sweep were no channel activity was detected from each individual sweep-exhibiting channel activity. The reconstructed macroscopic current subsequently was obtained by summing the resulting 50 to 60 recordings.

LITERATURE CITED

Amtmann A, Jelitto TC, Sanders D (1999) K^+-Selective inward-rectifying channels and apoplastic pH in barley roots. Plant Physiol **119:** 331–338

Amtmann A, Laurie S, Leigh R, Sanders D (1997) Multiple inward channels provide flexibility in Na^+/K^+ discrimination at the plasma membrane of barley suspension culture cells. J Exp Bot **48:** 481–497

Cosgrove DJ, Hedrich R (1991) Stretch-activated chloride, potassium, and calcium channels coexisting in plasma membranes of guard cells of *Vicia faba* L. Planta **186:** 143–153

Delhaize E, Craig S, Beaton CD, Bennet RJ, Jagadish VC, Randall PJ (1993a) Aluminum tolerance in wheat (*Triticum aestivum* L.): I. Uptake and distribution of aluminum in root apices. Plant Physiol **103:** 685–693

Delhaize E, Ryan PR, Randall PJ (1993b) Aluminum tolerance in wheat (*Triticum aestivum* L.): II. Aluminum-stimulated excretion of malic acid from root apices. Plant Physiol **103:** 695–702

Dietrich P, Hedrich R (1998) Anions permeate and gate GCAC1, a voltage-dependent guard cell anion channel. Plant J **15:** 479–487

Findlay GP, Tyerman SD, Garrill A, Skerret M (1994) Pump and K^+ inward rectifiers in the plasmalemma of wheat root protoplasts. J Membr Biol **139:** 103–116

Frachisse JM, Thomine S, Colcombet J, Guern J, Barbier-Brygoo H (1999) Sulfate is both a substrate and an activator of the voltage-dependent anion channel of *Arabidopsis* hypocotyl cells. Plant Physiol **121:** 253–261

Gassmann W, Schroeder JI (1994) Inward-rectifying K^+ channels in root hairs of wheat: a mechanism for aluminum-sensitive low-affinity K^+ uptake and membrane potential control. Plant Physiol **105:** 1399–1408

Hamill OP, Marty A, Neher E, Sakmann B, Sigworth FJ (1981) Improved patch clamp techniques for high resolution current recording from cells and cell-free membrane patches. Pflueg Arch **391:** 85–100

Hedrich R, Busch H, Raschke K (1990) Ca^{2+} and nucleotide dependent regulation of voltage dependent anion channels in the plasma membrane of guard cells. EMBO J **9:** 3889–3892

Hedrich R, Marten I (1993) Malate-induced feedback regulation of plasma membrane anion channels could provide a CO_2 sensor to guard cells. EMBO J **12:** 897–901

Ilan N, Schwartz A, Moran N (1994) External pH effects on the depolarization-activated K^+ channels in guard cell protoplasts of *Vicia faba.* J Gen Physiol **103:** 807–831

Iwasaki I, Arata H, Kijima H, Nishimura M (1992) Two types of channels involved in the malate ion transport across tonoplast of a Crassulacean acid metabolism plant. Plant Physiol **98:** 1494–1497

Kochian LV (1995) Cellular mechanisms of aluminum toxicity and resistance in plants. Annu Rev Plant Physiol Plant Mol Biol **46:** 237–260

Köhler B, Raschke K (2000) The delivery of salts to the xylem: three types of anion conductance in the plasmalemma of the xylem parenchyma of roots of barley. Plant Physiol **122:** 243–254

Ma JF, Zheng SJ, Hiradate S, Matsumoto H (1997a) Detoxifying aluminum with buckwheat. Nature **390:** 569–570

Ma JF, Zheng SJ, Matsumoto H (1997b) Specific secretion of citric acid induced by Al stress in *Cassia tora* L. Plant Cell Physiol **38:** 1019–1025

Ma Z, Miyasaka SC (1998) Oxalate exudation as a mechanism of aluminum tolerance in taro. Plant Physiol **118:** 861–865

Neher E (1992) Correction for liquid junction potentials in patch clamp experiments. Method Enzymol **204:** 123–131

Pantoja O, Gelli A, Blumwald E (1992) Characterization of vacuolar malate and K$^+$ channels under physiological conditions. Plant Physiol **100:** 1137–1141

Parker DR, Norvell WA, Chaney RL (1995) GEOCHEM-PC: a chemical speciation program for IBM and compatible computers. *In* RH Loeppert, AP Schwab, S Goldberg, eds, Chemical Equilibrium and Reaction Models. Soil Science Society of America, Madison, WI, pp 253–269

Pellet DM, Grunes DL, Kochian LV (1995) Organic acid exudation as an aluminum-tolerance mechanism in maize (*Zea mays* L.). Planta **196:** 788–795

Pellet DM, Papernik LA, Kochian LV (1996) Multiple aluminum resistance mechanisms in wheat: the roles of root apical phosphate and malate exudation. Plant Physiol **112:** 591–597

Piñeros M, Tester M (1995) Characterization of a voltage-dependent Ca^{2+}-selective channel from wheat roots. Planta **195:** 478–488

Piñeros M, Tester M (1997) Calcium channels in plant cells: selectivity, regulation and pharmacology. J Exp Bot **48:** 551–577

Roberts SK, Tester M (1995) Inward and outward K$^+$-selective currents in the plasma membrane of protoplasts from maize root cortex and stele. Plant J **8:** 811–825

Ryan PR, Delhaize E, Randall PJ (1995a) Characterization of Al-stimulated efflux of malate from the apices of Al-tolerant wheat roots. Planta **196:** 103–110

Ryan PR, Delhaize E, Randall PJ (1995b) Malate efflux from root apices: evidence for a general mechanism of Al-tolerance in wheat. Aust J Plant Physiol **22:** 531–536

Ryan PR, DiTomaso JM, Kochian LV (1993) Aluminum toxicity in roots: an investigation of spatial sensitivity and the role of the root cap. J Exp Bot **44:** 437–446

Ryan PR, Skerrett M, Findlay GP, Delhaize E, Tyerman SD (1997) Aluminum activates an anion channel in the apical cells of wheat roots. Proc Natl Acad Sci USA **94:** 6547–6552

Schachtman DP, Tyerman SD, Terry BR (1991) The K$^+$/Na$^+$ selectivity of a cation channel in the plasma membrane of root cells does not differ in salt-tolerant and salt-sensitive wheat species. Plant Physiol **97:** 598–605

Schmidt C, Schelle I, Liao YJ, Schroeder JI (1995) Strong regulation of slow anion channels and abscisic acid signaling in guard cells by phosphorylation and dephosphorylation events. Proc Natl Acad Sci USA **92:** 9535–9539

Schmidt C, Schroeder JI (1994) Anion selectivity of slow anion channel in the plasma membrane of guard cells: large nitrate permeability. Plant Physiol **106:** 383–391

Schroeder JI (1995) Anion channels as central mechanisms for signal transduction in guard cells and putative functions in roots for plant-soil interactions. Plant Mol Biol **28:** 353–361

Schroeder JI, Hagiwara S (1989) Cytosolic calcium regulates ion channels in the plasma membrane of *Vicia faba* guard cells. Nature **338:** 427–430

Schroeder JI, Keller BU (1992) Two types of anion channel currents in guard cells with distinct voltage regulation. Proc Natl Acad Sci USA **89:** 5025–5029

Schulz-Lessdorf B, Lohse G, Hedrich R (1996) GCAC1 recognizes the pH-gradient across the plasma membrane: a pH sensitive and ATP-dependent anion channel links guard cell membrane potential to acid and energy metabolism. Plant J **10:** 993–1004

Skerrett M, Tyerman SD (1994) A channel that allows inwardly-directed fluxes of anions in protoplasts derived from wheat roots. Planta **192:** 295–305

Terry BR, Findlay GP, Tyerman SD (1992) Direct effects of Ca^{2+}-channel blockers on plasma membrane cation channels of *Amaranthus* tricolor protoplasts. J Exp Bot **43:** 1457–1473

Terry BR, Tyerman SD, Findlay GP (1991) Ion channels in the plasma membrane of *Amaranthus* protoplasts: one cation and one anion channel dominate the conductance. J Membr Biol **121:** 223–236

Thomine S, Guern J, Barbier-Brygoo H (1997) Voltage-dependent anion channel of *Arapidopsis* hypocotyls: nucleotide regulation and pharmacological properties. J Membr Biol **159:** 71–82

Thomine S, Zimmermann S, Guern J, Barbier-Brygoo H (1995) ATP-dependent regulation of an anion channel at the plasma membrane of protoplasts from epidermal cells of *Arabidopsis* hypocotyls. Plant Cell **7:** 2091–2100

Tyerman SD (1992) Anion channels in plants. Annu Rev Plant Physiol Plant Mol Biol **42:** 351–373

Tyerman SD, Skerrett M, Garrill A, Findlay GP, Leigh RA (1997) Pathways for the permeation of Na$^+$ and Cl$^-$ into protoplasts derived from the cortex of wheat roots. J Exp Bot **48:** 459–480

Wegner LH, De Boer AH (1997) Properties of two outward-rectifying channels in root xylem parenchyma cells suggest a role in K$^+$ homeostasis and long-distance signaling. Plant Physiol **115:** 1707–1719

Wegner LH, Raschke K (1994) Ion channels in the xylem parenchyma of barley roots. Plant Physiol **105:** 799–813

White PJ, Lemtiri-Chlieh F (1995) Potassium currents across the plasma membrane of protoplasts derived from rye roots: a patch-clamp study. J Exp Bot **286:** 497–511

Zheng SJ, Ma JF, Matsumoto H (1998) High aluminum resistance in buckwheat: I. Al-induced specific secretion of oxalic acid from root tips. Plant Physiol **117:** 745–751

Zimmermann S, Thomine S, Guern J, Barbier-Brygoo H (1994) An anion channel current at the plasma membrane of tobacco protoplasts shows ATP-dependent voltage regulation and is modulated by auxin. Plant J **6:** 707–716